Updated November 18, 2017

Neutron Production with a 12-Inch Cyclotron

Timothy W. Koeth

ABSTRACT Neutron production from the $d(d,n)He^3$ reaction has been observed in the authors's 12-Inch Cyclotron[1]. The cyclotron's recent move to a new laboratory offered the necessary radiological controls to permit generation of fast neutrons. Since the cyclotron is intended for proton acceleration, the radio frequency was approximately halved to accommodate the q/m = ½ of deuterons. A solid target, prepared by loading a thick titanium plate with deuterium, was affixed to a radial probe and inserted into the vacuum chamber. The probe's radial position determined the incident deuterium beam energy. Neutrons were observed by several methods: direct detection, observation of nuclear excitations, and activation of metallic foils, and fission. This paper will highlight several crucial components and experiments to realize this operational milestone, which has elevated this cyclotron's status to a machine of nuclear physics.

INTRODUCTION Twenty years prior to this writing, the author's principal research interest was focused on nuclear physics in which a copious source of neutrons was required. Sealed neutron sources, such as an intimate mixture of radium-beryllium, posed several disadvantages including the radiological dangers in preparing and use of strong radium sources, the inability to 'shut off' the neutron production when no longer desired, and the expense of disposal. Other options were sought.

Accelerator-based neutron generation was found to be a more attractive method. On command, benign elements are made to fuse, expelling energetic neutrons. Further, the reaction ceases when the accelerator is de-energized. Many nuclear reactions produce neutrons, but perhaps the simplest is *d-d* reaction, with a broadly peaked cross section at a mere 180 keV. With an incident energy beam, in the regime of 180 keV, the reaction $d(d,n)He^3$ reaction produces 2.45 MeV neutrons quasi-isotropically.

Although distracted from the initial goal of this pursuit, having been happily lured into a successful accelerator physics career, the author never lost sight of that defining moment when two nucleons, under his command, would bring about the alchemist dream – at least a version of it.[2,3] This paper records the initial neutron generation by the author's 12-Inch Cyclotron.[4]

RF CONFIGURATION Primarily dedicated to proton acceleration, the cyclotron's Radio Frequency (RF) systems was retuned to 7.15 MHz to satisfy the magnetic resonance acceleration condition for deuterons having a q/m of half that of the single a.m.u. proton. A new, externally coiled, tank circuit inductor was wound to bring the DEE's 78 pF capacitance into resonance. The coupling loop was adjusted to present the RF power amplifier with a pure 50-ohm load.

A programmable Tektronix AFG3101 100 MHz arbitrary function generator supplied the RF drive and timing trigger output. The intermediate RF stage utilized a solid state ENI-350L which in turn drove the final power amplifier, an Ameritron AL-82 linear capable of 1500 Watts continuous. Lack of active DEE cooling limited the RF power to about 1000 watts average. When not in CW mode, pulsed RF operation was used to simultaneously achieve the highest DEE voltage possible while not exceeding the thermal tolerances. The upper trace in figure 1 displays the RF envelope, the lower trace beam current incident on the target. The observed roll off on the beam current signal is a consequence of the low pass filter transfer characteristic. The RF auto tuner was only employed during CW operation, as provisions have not been installed for pulsed operation.

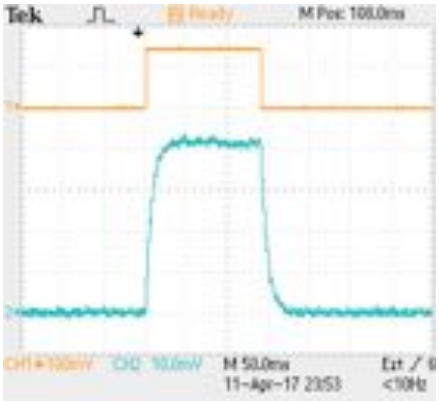

Figure 1 Oscilloscope trace of typical RF pulse: upper trace is the 140 ms RF envelope, the bottom trace is of a 40 nA peak beam current profile.

ION SOURCE & BEAM The cold cathode PIG ion source can provide beam currents as high as 1 μa, but a mixture of operational constraints limited the beam current on target to about 100nA or less.[5] Ion production linearly follows the PIG discharge up to 60 mA. However, a sustained discharge current greater than 30 mA leads to the negative impedance regime and an associated thermal runaway. In that regime, without water-cooling, the ion source would quickly suffer failure. Thus the ion source operation was limited to 20 mA discharge current. The gas flow had to be severely throttled because of the vacuum systems inadequate pumping speed; the chamber's operating pressure was maintained at 4E-6 Torr or less. The beam current on target quickly diminished at higher pressure. Finally, the radial profile of the ion's beam current falls off quickly with radius. Improvements in the ion source, vacuum system, and magnetic focusing will increase the beam current. The target, located at the end of a radial probe, is electrically isolated and connected to a BNC vacuum feed through. A short coaxial cable connected the target's signal to the input of oscilloscope's vertical amplifier. With 1MΩ input impedance, a 1μA beam current creates a 1V deflection. The rise time, as well as decay time noted in the beam current (lower) trace of figure 1 is an artifact of the RC response of the measurement circuitry, which utilized a low pass filter to suppress RF pickup from the DEE. The actual ion source current profile is prompt. The ion source chimney used, with a 1/32-inch diameter aperture, is displayed in figure 2.

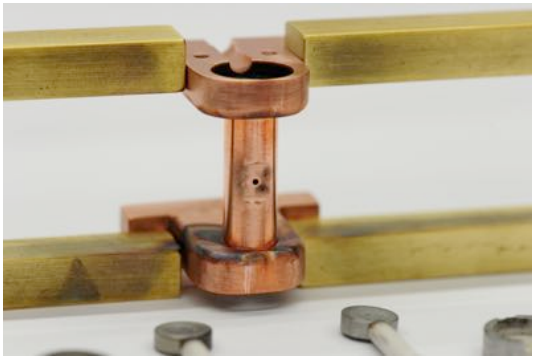

Figure 2. Cold cathode PIG ion source. Source aperture was 1/32-inch in diameter. (shown partially disassembled)

TARGET PREPARATION It is well known that titanium acts as a sponge for hydrogen. Properly prepared, titanium can be loaded in excess of 200% (atomic) with hydrogen; that is for every titanium atom two hydrogen atoms can be captured. After substantial loading, the titanium becomes very brittle from the immense effective internal pressures. The space program's extensive use of titanium for spacecraft required understanding of the embrittlement phenomena and subsequently produced abundant literature. A recipe for the controlled loading of titanium with hydrogen gas was adopted from Livanov, et al. [6]

The loading apparatus consisted of a clam-shell tube furnace capable of reaching 1000°C, into which was inserted a two foot quartz tube connected to a high-vacuum system. The vacuum system consists of a mechanically backed turbo pump that was supplemented with an in-line lN2 cold trap. It achieves an absolute vacuum pressure of $1x10^{-6}$ Torr at the distal end of the quartz tube. At that far end, pressure measurements were taken with an ion gauge mounted on a KF25 manifold. A photograph of the setup is shown in figure 3. A sequence of valves isolated the vacuum pump from the furnace region and permitted the back-filling of deuterium gas up to an atmosphere. A type-K thermocouple was inserted into the quartz tube and the junction was located at the center of the furnace region. Vacuum was maintained by a ceramic-metal vacuum feed through. The furnace temperature was automatically regulated to a programmed set point based on the thermocouple's readout.

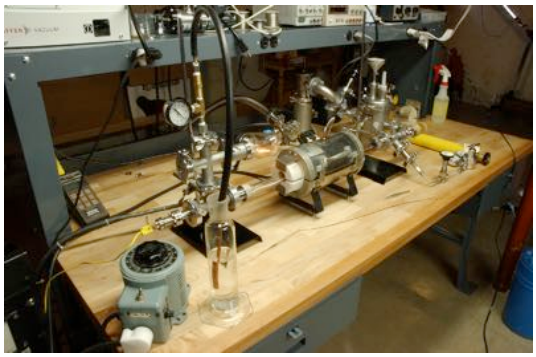

Figure 3. Apparatus for loading titanium with hydrogen.

Three identical samples were cut from a 0.010-inch thick sheet of laboratory grade titanium. Each sample was nominally 10 mm X 20 mm. They were cleaned with acetone and methanol. Precise mass measurements were made before the loading – these mass measurements included gases already adsorbed. Two of the three samples were loaded into center of the quartz tube, the vacuum system sealed and pumped. The third sample was kept as a reference.

A base vacuum of $1x10^{-6}$ Torr was established before heating the samples. Pressure measurements, plotted in figure 4, were made as the tube furnace warmed to 900°C and throughout the ~3 hour dwell period. As the temperature rose so did the pressure, indicating

outgassing. The pressure slowly dropped during the 900°C dwell. Once the pressure dropped to approximately $2x10^{-5}$ Torr, the vacuum pump was isolated and the tube furnace was quickly backfilled and maintained at one atmosphere of deuterium.

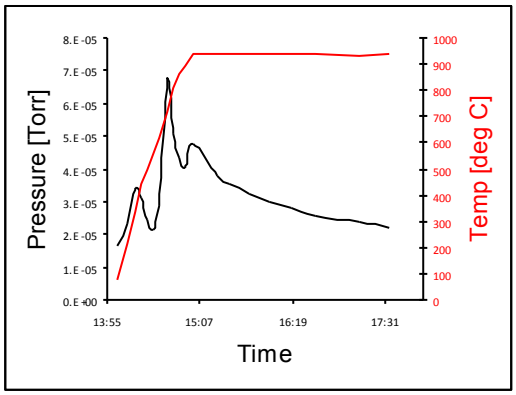

Figure 4. Vacuum tube furnace temperature (red) and pressure (black) during warm-up and dwell phases of the degassing.

A water bubbler connected to the manifold through a check valve was used to indicate a slight pressure above atmosphere within the quartz tube. The deuterium flow was set to cause approximately one bubble per second ensuring a slight positive pressure at all times. Audible 'crinkling' sounds were heard from the targets as the deuterium gas was introduced.

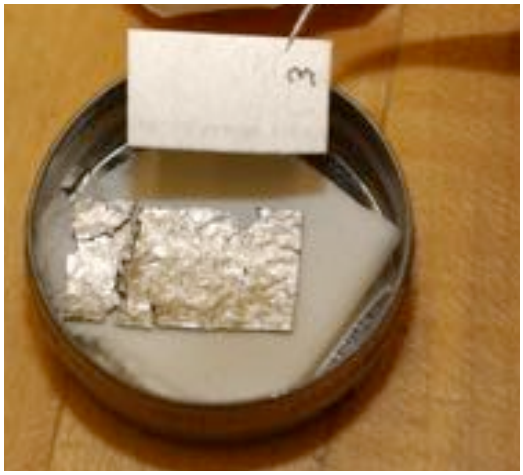

Figure 5. Comparison of two initially identical titanium samples. Swelling and embrittlement of the loaded sample is pronounced.

There was a notable delay between the start of the gas flow and the first bubbles. Once the bubbling began, it was assumed that the titanium targets were saturated and cooling could commence. The clam-shell tube furnace was de-energized, opened and lowered away from the quartz tube so as to quickly bring the samples back to room temperature, thereby locking the deuterium into the titanium plates. Deuterium flow continued until the targets were at room temperature. Visually, as seen in figure 5, it was clear that the targets had swelled, developed large grain structures and fissures.

After the loading, each target was again precisely massed, both indicating an increase of 56 mg. Table 1 summarizes the mass and dimensional increases. It is worthwhile to note that the compression of the same quantity of gaseous deuterium into a volume of the titanium sample would result in a pressure of 20,000 PSI! With that in mind, it is understandable that the titanium would swell. Determined by the mass measurements, greater than 220% (atomic) deuterium loading has been achieved in our samples.

parameter	before loading	after loading	**Δ**
#1, mass	0.61872 g	0.67515 g	**56 mg**
#1, height	12.24 mm	13.5 mm	10%
#1, width	21.75 mm	24.0 mm	10%
#2, mass	0.60395 g	0.66030 g	**56 mg**
#2, height	12.25 mm	13.5 mm	4%
#2, width	21.34 mm	22.34 mm	10%

Table 1. Summary of loaded titanium sample parameters

The targets were prepared in February of 2008, and were mounted to sample holders using a silver epoxy and were stored at atmosphere until their use in April 2017. Because of their attachment to the target holders, periodic mass measurements could not be taken, thus there is no knowledge of the deuterium retention. The loaded titanium sample, its mounting, and radial position inside the cyclotron chamber are shown in figure 6.

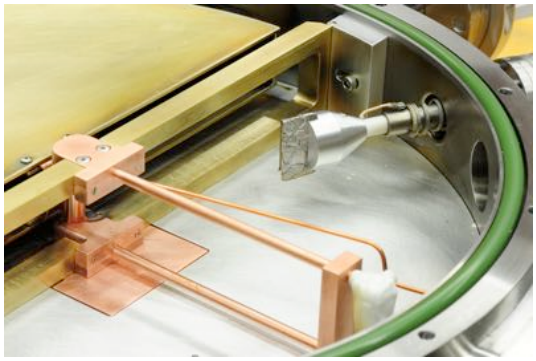

Figure 6. Deuterated target arrangement within the cyclotron chamber shown at the radial position found for maximum neutron production.

The Ti:D loading system will soon be reconfigured in the new cyclotron lab and fresh targets will enjoy a faster loading-to-beam turn around time.

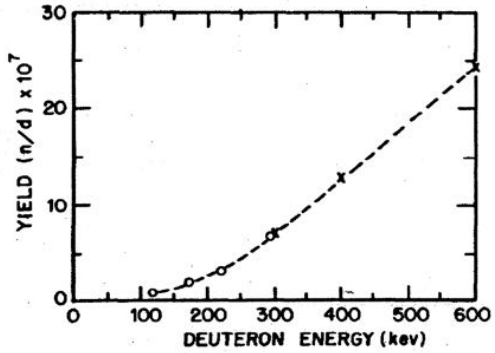

Figure 7. Neutron yield as a function of deuteron energy incident on a thick deuterated target – taken from Halpern [7]

NEUTRON PRODUCTION The cyclotron was tuned for maximum deuteron beam current on the radial probe, which was set to radius of 4 inches – this is just prior to the beam entrance into the deflection channel.[6] The probe was then fully retracted, allowing the beam to enter the deflection channel. A deflector voltage of 16 kV placed the deuteron beam onto the phosphor screen, confirming the energy at 250keV. After fine-tuning of the RF and magnetic field the beam's stability was monitored for a few minute period. Neutrons were not detected. Following the data of Halpern [5] on neutron yield for a given beam of a given current impinging thick deuterium targets, reprinted in figure 7, it was anticipated to see the onset of neutron production at energies as low as 100 keV. An increase in neutron fluence was expected with an increase in the targets radial position, necessarily associated with incident deuteron energy.

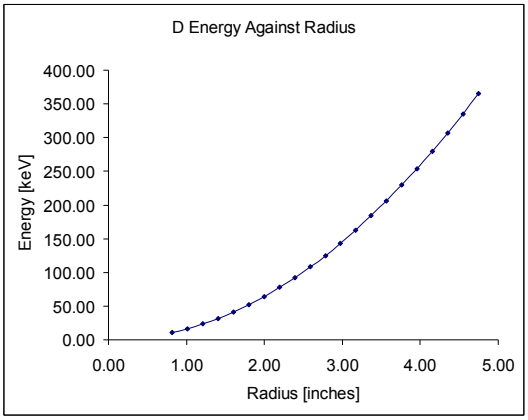

Figure 8. Calculated deuteron beam energy as a function of radius under nominal operating conditions

The radial probe was slowly inserted until neutrons were detected. The target position was adjusted for maximum measured neutron dose rate, which was found to be at a radius of 3 inches, for an inferred energy of 150 keV with a measured beam current of 100nA, as respectively depicted in figures 8 and 9. This was the crossover point of increasing beam energy and decreasing beam current.

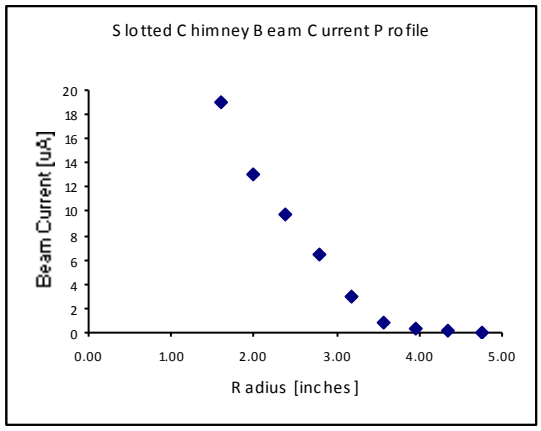

Figure 9. Measured beam current profile as a function radius under typical operating conditions.

NEUTRON DETECTION Three independent and different style portable neutron detectors simultaneously verified the presence of neutrons. The primary detector was a Ludlum Model 12-4 boron-10 enriched BF_3-tube based 'rem ball' with a scalar option. The 12-4 is calibrated for dose and thus the meter's units display mrem/hour. While not as sensitive as the other two tubes, the 12-4 was the primary diagnostic as its BF_3 tube was unaffected by the magnetic field and could be positioned arbitrarily close to the cyclotron chamber. The second and third detectors were photomultiplier based detectors; one being a Ludlum Model 42-4 LiF(Eu) scintillator, and the third detector a Ludlum Model 42-2 proton recoil detector. When positioned sufficiently far away from the cyclotron magnet, neutrons were detected by both, however, an approach closer than two feet of the magnet gap either greatly reduced or otherwise extinguished the photomultiplier tube signals.

All three detectors responded in unison for the duration of each pulse when operating in RF pulse mode. Several tests were performed to ensure the detectors' response were to neutrons. First, the target was inserted so as to only intercept the low energy deuterons – the detectors ceased their counting. Second, with the target the position of greatest production rate, the ion source was gas starved, beam current decreased as well as the measured neutron dose rate. Finally, the cyclotron's magnetic field was slightly adjusted to break the optimized magnetic resonance acceleration condition, and again the neutron fluence followed the diminishing beam current.

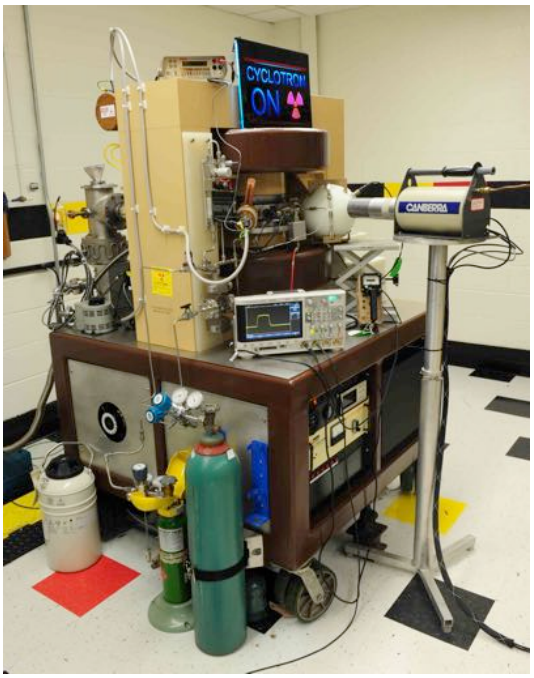

Figure 10. Ludlum Model 12-4 BF_3 detector arrangement. The center of the detector was 29.5 cm from the Ti:D target. A high resolution HPGE gamma ray spectroscopy detector sits atop an aluminum stand, about 36 inches away from the target. Note the green deuterium gas supply bottle at bottom-left.

The 12-4's nine-inch 'rem ball,' shown in figure 10, was placed as close as possible to the target by nesting it between the top and bottom magnet coils and next to the radial probe's actuator, such that the sensitive element sat in the median plane. At this location the 1.6 cm diameter X 2.5 cm tall BF_3 tube was 29.5 cm away from the target. Assuming the most favorable orientation of the cylindrical BF_3 tube, the maximum area of the detector is taken to be 4 cm^2; the actual effective area may have been as much as one half that, or 2 cm^2. Sitting at a radius of 29.5 cm, the tube only intercepted 4 cm^2 out of the available 10,930 cm^2 4π spherical surface – yielding a geometrical efficiency of $3.7x10^{-4}$.

With an RF duty factor of 25% (RF on for 125 ms twice a second) an average dose rate of 20 mrem/hour was measured. Using the health physics standard of 8.2 n/sec/cm^2/mrem/hour for 2.45 MeV neutrons, a peak isotropic neutron production of 10 million neutrons per second can be inferred.

The average dose rate increased linearly with the RF pulse repetition rate. The duty factor was briefly raised to 100% where the measured average dose rate reached 80 mrem/hr. A screen shot of the RF/Beam monitoring oscilloscope, figure 11, shows 80 nA peak deuteron beam at about 50% duty factor.

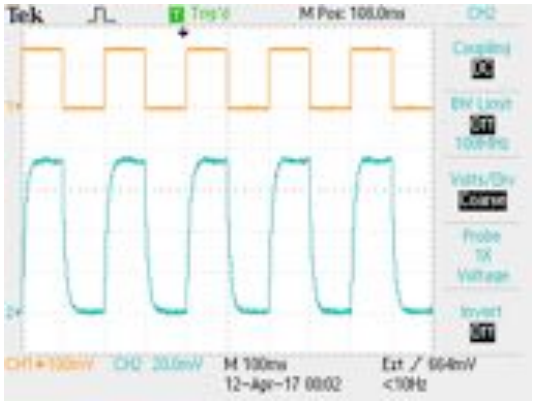

Figure 11. Oscilloscope screen shot of an increased RF pulse repetition rate (yellow trace) and corresponding beam current on target (blue trace) – 80 nA peak.

NEUTRON ACTIVATION An unequivocal indication of neutron production is the radio-activation of metallic foils. Silver and indium foils were exposed to the cyclotron's neutrons, inducing short-lived radioactive isotopes in them. After the neutron irradiation, the foils' induced radioactivity was recorded by a Geiger-Mueller (G-M) counter in time bins much shorter than the isotopes' half-lives until the activity fell to background rates. The principle activations of silver include Ag^{110} and Ag^{108}; both beta decay via the process ${}^1_0n \rightarrow {}^1_1p + e^- + \nu^0$ to Cd^{110} and Cd^{108} respectively. The half-life of Ag^{110} is 24.6 seconds; the half-life of Ag^{108} is 2.42 minutes. Their short half-lives quickly bring them to equilibrium during irradiation, however, they make the subsequent decay measurements challenging. Indium is also commonly used for activation analysis. In^{115} → In^{116m} is a metastable state with a 54.2 minute half-life, thus requiring a longer irradiation time, and of course, improving the decay measurement.

The energetic neutrons of the d-d reaction must be moderated to thermal energies to before the can be absorbed by the target nuclei. The foils were taped to a 45 mm thick polyethylene moderator and placed directly outside of the glass view port which was the nearest to the Ti:D target. A Ludlum Model 44-40 lead-shielded Geiger-Muller pancake probe was positioned to monitor the foils' activity buildup; however it also measured activity from the myriad gamma rays, which serendipitously provided a record of the cyclotron's beam tune-up.

The irradiation time of the silver was approximately 10 minutes. While the silver foil's irradiation showed definite activation, it quickly decayed to levels indiscernible against background. Figure 12 shows the decay of Ag^{110}, but the Ag^{108} signal is comparable to background level.

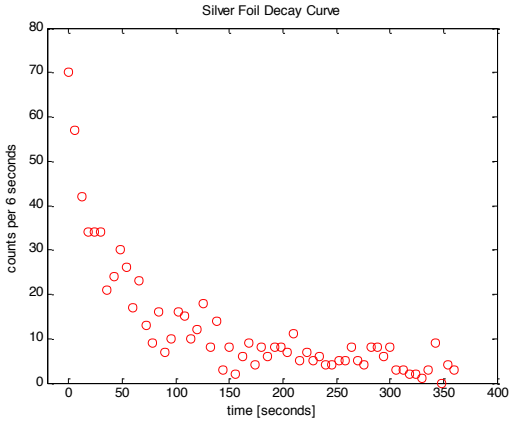

Figure 12. Decay curve of neutron activated silver foil. Each measurement time bin is six seconds.

The indium foil activation produced more satisfying results. The irradiation time of the indium foil was approximately 6.5 minutes, a fraction of the time needed to achieve activation saturation; yet, the peak-induced activity was at an order of magnitude above background. The indium decay data was re-binned into 1-minute increments, substantially improving the statistics, and is plotted in Figure 13. The linearity of the same data plotted on a semi-log plot, as displayed in the lower graph of figure 13, indicates the isotopic purity of the indium foil.

Theoretical decay curves were plotted on top of the indium decay raw count data of figure 13. The theoretical curve is a single exponential decay constant, with a half-life of 54.2 minutes, with initial count rate of 153 counts per minute above a background of 24 counts per minute.

Using a portable shielded high-resolution High Purity Germanium (HPGe) gamma ray spectrometer was positioned to record a timed sequence of spectroscopy data on the indium foil. The seven gamma ray lines observed, (138, 416, 818, 1097, 1293, 1507, 2112 keV) belong to ^{116m}In, which has a half life of 54.2 minutes.

NEUTRON INDUCED GAMMA RAYS

NaI(Tl) measurements: As the energetic neutrons interact with their surroundings, a plethora of gamma rays are generated. At first a NaI(Tl) based gamma ray spectrometer was installed near the cyclotron. Unfortunately the gain of the detector's photomultiplier tube was severely decreased by the magnetic field. Even with a mu-metal shield installed over the detector, if it was placed too close to the cyclotron magnet, the signal completely ceased. A location was determined through a compromise between detector signal and measurable gamma ray flux. The detector was placed approximately three feet away from the Ti:D target seen in figure 10.

Once the cyclotron beam was tuned for maximum neutron production, the magnetic field was set and not adjusted further. The gamma ray spectrum was first gathered with beam on for 793 seconds, followed by a beam-off (RF off) background run of exactly the same detector live time for subtraction. Also under the same magnetic field conditions, two beam-off runs were performed with radioactive sources Co^{60} and Cs^{137} in the detector's presence for energy calibration.

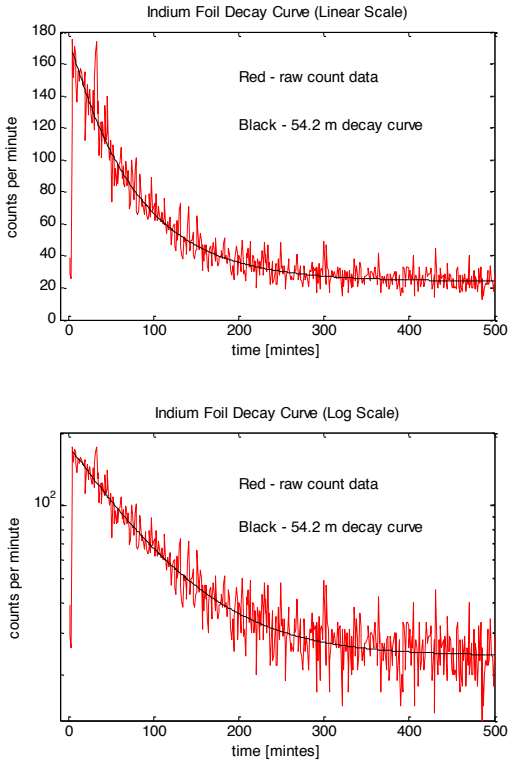

Figure 13. Linear (top) and semi-log (bottom) decay curves of neutron activated indium foil.

While it is difficult to track down and identify all of the interactions, two of the expected gamma ray lines are telltale evidence of neutron production, and can be seen in the spectrum of figure 14.

The first is an 847 keV gamma line that comes from inelastic scattering of the neutron with magnet's iron nuclei. Consistent with that line, our measurements display an 847 keV+/- 10% peak. The second line expected and observed is a 2.22 MeV gamma ray from the proton capture of a neutron; it is the binding energy released during the creation of a deuteron. This occurs in hydrogenous material, such as the polyethylene moderator used in the foil activation experiments as well as the Bonner sphere of the Ludlum Model 12-4 neutron 'rem ball' detector.

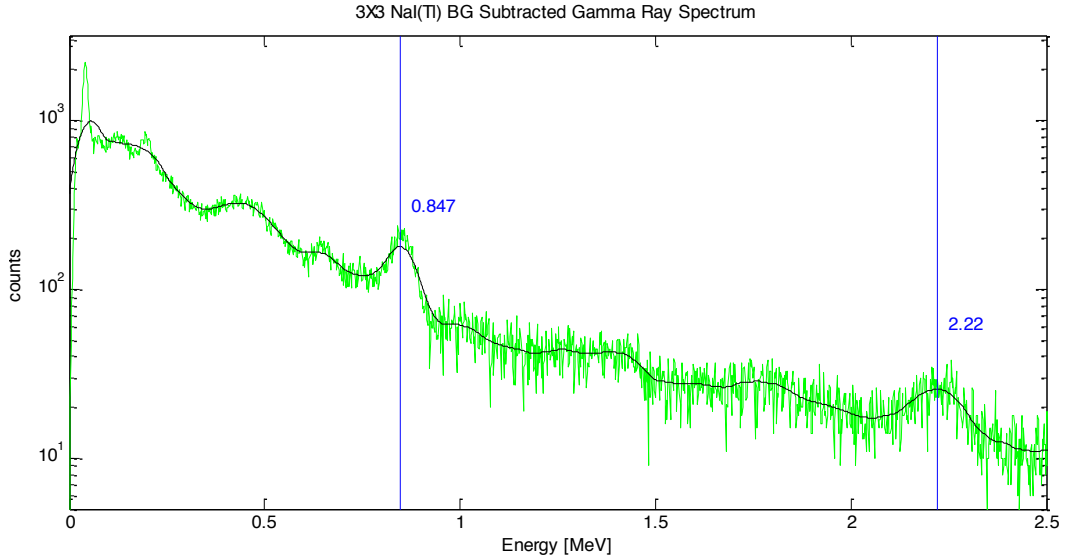

Figure 14. NaI(Tl) background subtracted gamma ray spectrum from a 13-minute data collection run. The green trace displays the raw data; the black trace is smoothed.

HPGe measurements: Motivated by the numerous unidentifiable lines in the NaI(Tl) measurement, a portable high-resolution High Purity Germanium (HPGe) gamma ray spectroscopy system was subsequently placed near the cyclotron during a "beam-on-target" run. This data collection time was minimized so as to minimize to neutron damage to the germanium detector. There was enough signal from a 6.5 minute "gated" run to reveal many more neutron induced gamma rays lines. The HPGe Multi-Channel Analyzer was gated in synchronization with the RF pulse, so as to only collect data during the "beam-on" period. Again, the 847keV and 2.22MeV lines are the prominent peaks, the additional gamma ray lines originate in the cyclotron's construction materials, such as 472, 1015keV lines from the aluminum chamber lid, and the 962keV line of copper, from the copper magnet coils. Several gammas lines, i.e. 140, 198, 596keV originate in the germanium of the gamma ray detector itself.

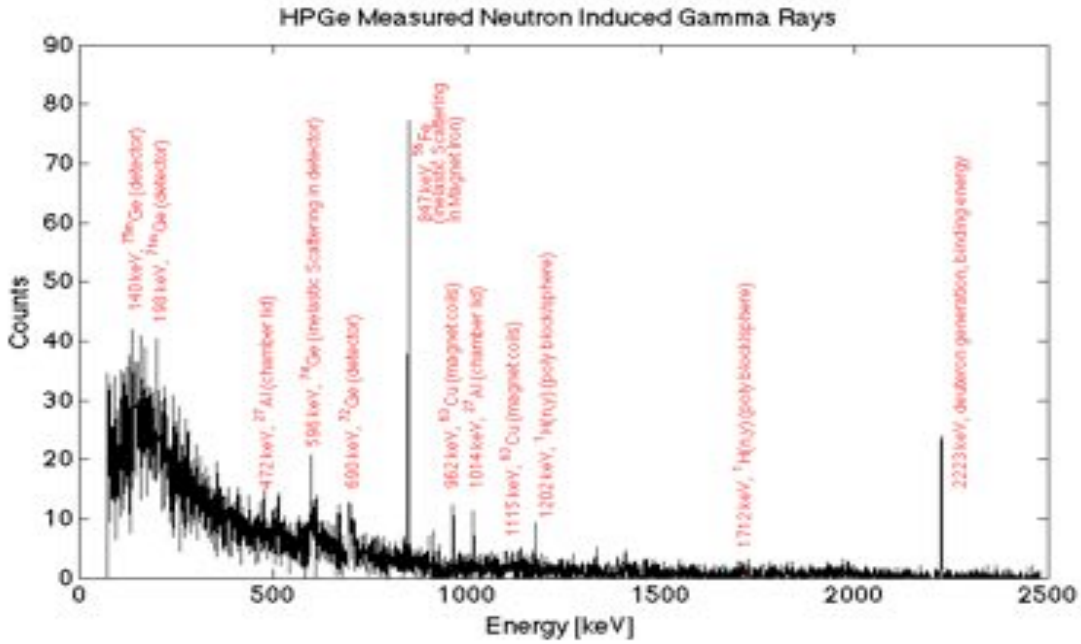

Figure 15. Background subtracted gamma ray spectrum from a 6.5 minute gated beam-on-target run.

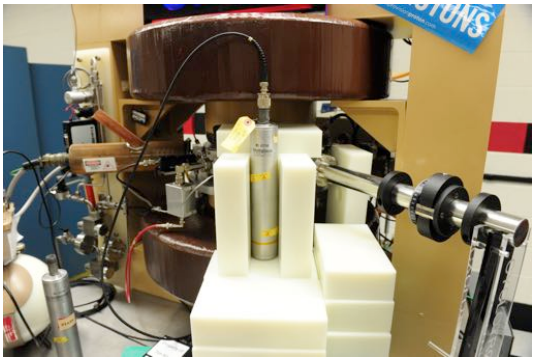

Figure 16. WL6376A Fission Chamber, surrounded by polyethylene moderator, placed near cyclotron chamber (some blocks removed to show tube) for neutron detection.

FISSION FROM FUSION The first demonstration of fission in the United States was performed by Fermi & Dunning at Columbia University cyclotron in Pupin Hall January 25, 1939. They mounted uranium inside an ion chamber and placed the assembly near the cyclotron. Neutrons generated by the cyclotron fissioned the uranium nuclei, and the subsequent energetic fission products created a large pulse of ionization that could be measured on an oscilloscope.

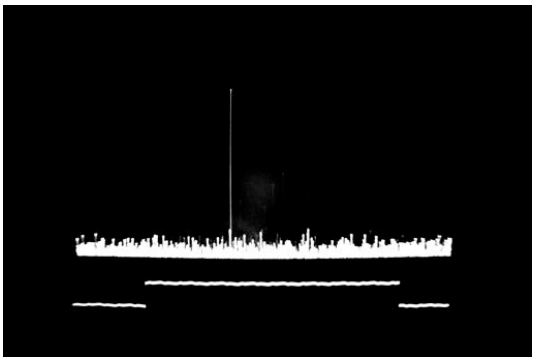

Figure 17. Upper trace: signature pulse of ionization from ^{235}U fission by the author's cyclotron. Lower trace: RF pulse.

Fission was similarly demonstrated with this 12-inch cyclotron to, in a sense, complete the set of discoveries brought forth by the 1930's cyclotrons. For this demonstration, a fission chamber was surrounded with moderating polyethylene blocks and placed next to the cyclotron's target region. The fission chamber used was a spare Westinghouse WL6376A, HEU ^{235}U lined tube intended for reactor nuclear instrumentation. Approximately 1 gram of ^{235}U lined an argon-filled proportional tube. The detector bias and signal are split with a preamp, the HV bias was +1100 V, the signal was conditioned with a pulse shaping spectroscopy amplifier, and distributed to an oscilloscope for observation and scalar/timer for counting. The tube placement, with several poly blocks removed for clarity, is shown in figure 16.

The cyclotron was tuned for maximum neutron production using a substantially more sensitive ^{3}He detector. Once neutron production was optimized, signal from the fission chamber was apparent. Similar to Fermi's experience, a large pulse appeared on the oscilloscope signifying a fission event, figure 17. These occurred at a rate of approximately 1 fission event per RF pulse.

FUTURE A vista of interesting experiments and processes are now possible with a controlled source of neutrons. Perhaps the most interesting procedures will be neutron-activation based techniques for isotope identification. Very short lived isotopes can be investigated by utilizing the pulsed RF operation. Further, other low energy nuclear reactions will be explored, such as the $F^{16}(p,\alpha)O^{16}$ reaction which is accompanied by energetic gamma rays. Efforts continue to improve the beam intensity and focusing, so as to minimize the beam current loss at the larger radii in the aim of further increasing the neutron fluence.

CONCLUSIONS Settling a personal pursuit for the author, a small 1 MeV proton cyclotron, modified to accelerate deuterons up to 400 keV, has demonstrated the ability to generate neutrons through the $d(d,n)He^3$ reaction. These neutrons have, in turn, interacted with the nuclei of surrounding material inducing measurable nuclear excitations and have fulfilled the alchemist's dream by radio-activating metallic targets whose decay yield elements, previously not present. Finally, in a first of any "amateur" cyclotron, this machine has demonstrated the fission of ^{235}U. These milestones have conferred upon the cyclotron and its creators the sorcery of nuclear physics!

REFERENCES

[1] T. Feder, "Building a cyclotron on a shoestring," *Physics Today*, November 2004

[2] C. Alter, "Accelerated Learning," *Washington Post Magazine*, September 11, 2016

[3] T. W. Koeth, "Beam Physics Demonstrations with the Rutgers 12-Inch Cyclotron" WEPPT025, *Proceedings of Cyclotrons 2013*, Vancouver, BC, Canada September 2013

[4] T.W. Koeth, "Undergraduate Education with the Rutgers 12-Inch Cyclotron," CAARI 2014, *Physics Procedia*

[5] T. W. Koeth, et. al, "Rutgers 12-Inch Cyclotron: Dedicated to Training Through R&D," WEPPT024, *Proceedings of Cyclotrons 2013*, Vancouver BC, Canada, September 2013

[6] V.A.Livanov, A.A. Bukhanova, and B.A. Kolachev, "Hydrogen in Titanium" Israel Program for Scientific Translations, Jerusalem 1965. Part 3, Chapter 1.

[7]J. G. Beckerley, "Neutron Physics – A Revision of I. Halpern's Notes on E. Fermi's Lectures in 1945," AECD-2664, Oct 16, 1951